# Barx2 functions through distinct corepressor classes to regulate hair follicle remodeling

**Lorin E. Olson*†, Jie Zhang*, Havilah Taylor*, David W. Rose‡, and Michael G. Rosenfeld*‡§**

*Howard Hughes Medical Institute, †Biomedical Sciences Graduate Program, and ‡Department of Medicine, Division of Endocrinology, University of California at San Diego School of Medicine, La Jolla, CA 92093-0648

Contributed by Michael G. Rosenfeld, January 20, 2005

**The hair-growth cycle, a complex biological system requiring coordinate alterations in gene expression and cellular behavior, provides a challenging model for investigating the interplay of specific transcriptional regulation events. Here we report that the Barx2 homeodomain factor serves as a regulator of hair follicle remodeling (catagen), and loss of *Barx2* in mice causes a defect both in the initiation and progression of catagen, resulting in a protracted first catagen, and later, causing short hair in adult gene-deleted mice. Barx2 negatively regulates its own promoter, and our study highlights the role of Barx2 as a repressor in the skin that can, unexpectedly, functionally interact with two WD40-domain factors distantly related to the yeast corepressor Tup1. These two corepressors, transducin-like enhancer of split and transducin β-like 1, function through distinct and independent interactions with Barx2 for the repression of gene targets, including the *Barx2* gene itself, emphasizing the roles of complementary repression strategies in engrailed homology-1 motif-containing homeodomain factors. Together, our data suggest that the hair-remodeling defect of *Barx2* mutant mice could be explained, in part, by failure to repress one or more critical target genes.**

hair cycle | TBL1 | TLE | transcriptional repression

A distinctive feature of the hair follicle is its periodic regeneration and degeneration throughout the lifetime of the organism in cycles of three phases: anagen, catagen, and telogen. In mice, hair follicle morphogenesis begins late in development and continues through growth, or anagen, of the first pelage until ≈2 weeks after birth. The final length of the hair is genetically determined by the period spent in anagen, with hair-generating cells of the bulb having a finite proliferative capacity that is influence by factors from the dermal papilla and surrounding tissues. Anagen terminates with the destruction of the growing part of the follicle in a remodeling process called catagen. Thereafter, a resting period, or telogen, intervenes with the finished hair normally retained in the diminutive follicle, until anagen reinitiates with the start of a new cycle of hair growth (1, 2). Two synchronous cycles of hair growth occur in juvenile mice, with consecutive waves of anagen–catagen–telogen moving from neck to tail, and thereafter only smaller patches of follicles cycle together in adult mice. From the human perspective, hair follicle remodeling is important because changes in the hair cycle underlie most disorders involving unwanted hair growth or loss (3, 4). Evidence is also emerging that hair cycling and wound healing share some basic molecular strategies (5).

The transcriptional control of skin and hair development, and regulation of postnatal, cycling hair follicles, represents a complex system involving the coordinated actions of many intracellular signaling molecules and transcription factors. Recently, expression profiling has been used to systematically identify hair-cycle-associated genes and cluster them into major classes of expression over the hair growth cycle (6); however, it remains unclear how these genes are regulated in a cyclic fashion and what their specific roles might be.

Expression of ovine *Barx2* has been shown in embryonic ectoderm and in the outer root sheath of mature wool follicles (7), but its role in skin and hair biology has not been defined. Barx2 is a homeodomain factor of the *Bar* family, sharing conserved, atypical residues with the homeodomains of *Drosophila* BarH1 and BarH2. In mammals, this family is divided into two groups: the *BarH*-like group of *BarHl1* and *BarHl2*/*MBH*, which are most similar in sequence to the *Drosophila Bar* genes (8, 9), and the *Barx* group including *Barx1* and *Barx2* (10, 11). Very little is known about the role of Barx2 in development, although functional studies in a cell culture system indicate that it can promote muscle differentiation (12). Here, using gene knockout technology, we report that Barx2 is required for normal progression of the catagen phase of the hair cycle and that it represses its own promoter in the epidermis and hair follicle.

Transcription factors mediate gene regulation by association with a coregulatory apparatus to alter chromatin structure or to interact with the general transcription machinery. All members of the *Bar*-homeodomain family have one or more N-terminal engrailed homology-1 (eh-1) motifs, which are generally recognized as recruitment points for TLE/Groucho-related factors. Mammalian homologs of *Drosophila* Groucho have been repeatedly identified as important corepressors for homeodomain proteins and other transcription factors (13–18). In the skin, TLE/Groucho factors acting through Tcf3 have been implicated in suppressing the terminal differentiation of epidermis (19). Four of the mammalian homologs, the transducin-like enhancer of split (TLE 1–4), contain C-terminal WD40 repeats that are involved in protein–protein interactions and thought to be important for repression. A second type of WD40-domain factors, the transducin β-like 1 (Tbl1) and a related factor (TblR1), have been linked to repression by unliganded nuclear receptors (20–23), and are required for corepressor–coactivator exchange during regulated gene activation events (24). Here, we provide the initial evidence that Tbl1 can function as a corepressor for a homeodomain factor, acting redundantly or cooperatively with TLE/Groucho factors in repressing Barx2 target genes.

## Materials and Methods

**Targeted Mutation of Barx2, Microarray Experiment, siRNA Sequences, and Primer Sequences for RT-PCR.** For details, see *Supporting Text*, which is published as supporting information on the PNAS web site.

**Histology and X-Gal Staining.** Embryos or tissues were fixed in 4% paraformaldehyde or fresh frozen in 1:1 OTC/aquamount and cryosectioned at 16 μm. For skin histology at time points between postnatal day 6 (P6) and P30, dorsal skin was taken from mouse littermates and separated into three segments (anterior, middorsal, and posterior) for sectioning. Some slides were stained with X-Gal for 12 h following standard protocols.

Abbreviations: TLE, transducin-like enhancer of split; Tbl1, transducin β-like; P*n*, postnatal day *n*; E*n*, embryonic day *n*; eh-1, engrailed homology 1.

§To whom correspondence should be addressed. E-mail: mrosenfeld@ucsd.edu.





www.pnas.org/cgi/doi/10.1073/pnas.0500519102

Thrombospondin-1 protein was detected with biotinylated anti-Tsp (NeoMarkers Ab-4).

**Hair-Length Measurement.** Pelage hairs were plucked from the middle of the back at P25 for juvenile hair-length measurements, or at 8 months for adult measurements, using 50 guard hairs from each of two *Barx2*$^{+/-}$ and two *Barx2*$^{-/-}$ mice.

**Primary Keratinocyte Culture, Transfection, and Nuclear Microinjection Assays.** Primary murine keratinocytes were isolated from newborn pups (1–3 days old) and maintained in an undifferentiated state according to the method of Dlugosz *et al.* (25). Cotransfection assays were performed with Fugene6 (Roche Diagnostics) by using 750 ng of luciferase reporter, 50 ng of pCMX expression plasmid, and 500 ng of pRSV$\beta$Gal as an internal control for transfection efficiency. The 3xBx/tk reporters were generated by multimerization of annealed oligonucleotides containing a consensus Barx2 binding site: TCTAATGGTTTTT (26). The Barx2 cDNA was cloned by PCR from an embryonic pituitary cDNA library and conformed to the full-length Barx2b isoform described by Herring *et al.* (27). Microinjection of reporter plasmids, IgG-purified antibodies (a pan-TLE antibody H321, Santa Cruz Biotechnology), siRNAs, and analysis was performed as described (24, 28). All transfections and microinjection experiments were performed at least twice.

**GST-Affinity Purification and Coimmunoprecipitation Assays.** GST-Barx2N′ for protein interactions was expressed in *Escherichia coli* with a Barx2 cDNA fragment encoding amino acids 1–132 (27) with either a wild-type eh-1 sequence or a 3-aa change at positions 25–27 generated by site directed mutagenesis (Stratagene). For Western blotting, we used anti-TLE3 (M201, Santa Cruz Biotechnology), anti-TLE1 (M101, Santa Cruz Biotechnology), or anti-N-CoR (28).

**Chromatin Immunoprecipitation (ChIP).** Full-thickness skins were minced with scissors and cross-linked for 1 h in 1% formaldehyde at room temperature. Tissue was then homogenized in lysis buffer and sonicated to shear fragments to the average size of 500–1,000 bp. Immunoprecipitation was performed with anti-Barx2 (Santa Cruz Biotechnology), anti-TLE (H321, Santa Cruz Biotechnology), anti-TLE1 (M101, Santa Cruz Biotechnology), anti-Tbl1 (24), and anti-N-CoR (28). 30 cycles of PCR were performed with primers surrounding the Barx2 sites at −1.6/−1.4 kb from the *Barx2* gene (ChIP primer sequences GAGAAATCAGGCAGAGGCAG and CCGGTGGTTAAACTCGCTAA).

**RNA Isolation and Real-Time PCR.** Total RNA was isolated from P11 skin with a RNeasy kit (Qiagen), and cDNA was synthesized by using a SuperScript kit (Invitrogen). Real-time PCR was performed on an AB17700 thermal cycler: 95°C for 15 min, then 45 cycles of 95°C for 10 s, 60°C for 1 min. Reactions (20 $\mu$l) included 2 $\mu$l of cDNA, target-specific primers, and CyberGreen mastermix (Qiagen). Quality and quantity of template was controlled by normalization to *Gapdh*. Reactions were performed in triplicate, and final results were found by using a relative standard curve.

## Results and Discussion

**Expression of Barx2 in Differentiating Stratified Epithelia and Targeted Mutation of Barx2.** Early developmental expression of *Barx2* has been reported for embryonic day 9.5 (E9.5) to E12.5 (11), including in the anterior pituitary gland from E12.5 in a spatial distribution resembling that of the pituitary developmental regulator, Pit1. We detected high levels of *Barx2* after E13.5 in Rathke's pouch, conjunctiva, cornea, tongue, mouth, nasal epithelium, esophagus, salivary gland, vibrissae, and skin by *in situ* hybridization (data not shown). Interestingly, in some structures (i.e., tongue, esophagus, and skin) *Barx2* was expressed in both the epithelium and underlying muscle but not in the intervening dermal/mesenchymal components (Fig. 1*A* and data not shown). At P8, we observed *Barx2* expression in the interfollicular epidermis and in the outer root sheath of hair follicles, and no expression in the follicular bulb (Fig. 1*B*), similar to what has been described for ovine wool follicles (7).

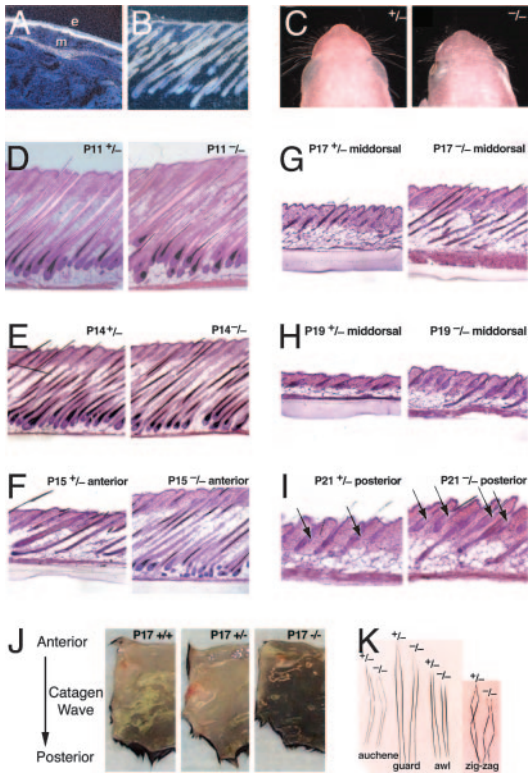


**Fig. 1.** *Barx2* mutant phenotypes: open eyelids and short whiskers at birth, defective juvenile hair follicle remodeling, and short adult hair. (*A*) Expression of *Barx2* mRNA in rump skin at E14.5 detected by *in situ* hybridization, with expression in epidermis (e) and underlying muscle (m). (*B*) *Barx2* expression in epidermis and outer root sheath of hair follicles at P8. (*C*) Two-day-old pups with short whiskers and open eyelids in mutants. (*D*) Follicles in full anagen with no difference between mutant and control. (*E*) Follicles at the anagen–catagen transition with no morphological differences. (*F*) Follicles with catagen morphology for control, but delayed at anagen–catagen transition for mutant. (*G*) Follicles with late catagen morphology for control, but delayed at early catagen for mutant. (*H*) Follicles in telogen for control, but delayed with catagen morphology for mutant. (*I*) Higher magnification of follicles at telogen or early second anagen for control, but still in catagen with enlarged sebaceous glands (arrows) for mutant. (*J*) Delayed pigment change on the underside of *Barx2* mutant skin indicates an offset in the anterior to posterior remodeling wave. (*K*) All four hair types are shorter in 8-month-old *Barx2* mutants.

To understand the role of Barx2 in development, we designed a targeting vector to delete the Barx2 homeodomain and C-terminal sequences by homologous recombination in ES cells, leaving a 134-aa Barx2 epitope fused in frame to $\beta$-galactosidase (Fig. 6, which is published as supporting information on the PNAS web site). This mutation disrupts DNA binding and nuclear localizing capacity of the mutant Barx2 protein, and generates a reporter for X-Gal staining to monitor the activity of the promoter in mutant animals. We could not detect mRNA transcripts encompassing the homeodomain or C terminus in mutant tissue by using RT-PCR (Fig. 6). Hence, the mutational strategy abolished generation of a functional Barx2 protein.

*Barx2*$^{-/-}$ pups were distinguishable by their short whiskers,

DEVELOPMENTAL BIOLOGY

and 50% were born with open eyelids (Fig. 1*C*). *Barx2*$^{+/-}$ pups were phenotypically equivalent to *Barx2*$^{+/+}$ pups and did not display hair cycle alterations (see below); therefore, the mutation strategy did not produce a dominant-negative allele or an allele with detectable neomorphic properties.

**Defective Hair Follicle Remodeling and Short Adult Hair in *Barx2* Mutants.** After ≈2 weeks of normal hair growth, we noticed a transient disheveled appearance to the pelage of *Barx2* mutants, with hairs tending to stand erect rather than lie flat against the body (data not shown). To better understand the alterations affecting the *Barx2* mutant coat, we undertook a histological study of follicles and skin at intervals between P6 and P30. In this endeavor, we were careful to compare matched sections of dorsal skin from the same regions of the mice (i.e., separately comparing anterior, middorsal, and posterior sections), because catagen is known to proceed in an anterior to posterior wave during this time. Basic criteria for staging hair follicles based on morphology have been well described in the literature (29). We found no differences between mutant and control follicles during full anagen at P11 (Fig. 1*D*), or at the anagen–catagen transition at P14 (Fig. 1*E*). Hair follicle morphology began to diverge in anterior sections at P15 (Fig. 1*F*), with mutant follicles in position-matched sections appearing morphologically delayed (Fig. 1 *G* and *H*). Whereas control follicles in posterior sections involuted and completed remodeling by P19, mutant follicles in this location did not achieve telogen morphology until P22–P23 (Fig. 1*I* and data not shown). In addition, during the final stages of protracted catagen, mutant sebaceous glands were enlarged (Fig. 1*I* arrows). During the hair cycle, skin pigments are necessarily eliminated as hair follicles transition through catagen, and consistent with our histological observations, we observed a delay in the anterior to posterior clearing of pigments on the underside of *Barx2* mutant skin (Fig. 1*J*). Thus, the anterior to posterior remodeling wave was offset as a consequence of *Barx2* gene mutation, and this defect correlates with the disheveled coat in mutant mice.

We considered the possibility that *Barx2* mutants might have a delay in the anagen to catagen transition, in addition to the protracted catagen, which could produce longer hair and contribute to the appearance of the disheveled coat. For example, murine *Fgf5* mutants (angora) have hair that is 50% longer than normal due to an extension of anagen (30). Instead, we found that plucked guard hairs from *Barx2*$^{-/-}$ mice were actually slightly shorter at P25, although the difference was of questionable significance, leading us to believe that the growth period of the first anagen is not significantly changed by mutation of *Barx2*. Furthermore, as *Barx2*$^{-/-}$ mice aged beyond ≈6 months, their hair became markedly shorter (Fig. 1*K*). Plucked guard hairs from a mid-dorsal region of 8-month-old mice exhibited an average length of 1.19 ± 0 07 cm in heterozygotes compared with 0.98 ± 0.07 cm in mutants ($P < 0.01$), for a difference of 15–20%. We did not observe broken hairs during our measurements. The late appearance of this phenotype may arise because adult anagen periods become progressively shorter in gene-deleted mice, coupled with the gradual shedding (exogen) of normal sized hairs. Based on their opposite effects on hair length, we suggest that Barx2 and Fgf5 have opposing roles in regulating hair growth, such that Fgf5 signals the end of anagen and Barx2 functions to prolong anagen in the adult pelage.

***Barx2* Gene Autorepression in Skin and Functional Interaction with Two Classes of WD Domain Corepressors.** We used the *Barx2-lacZ* knock-in allele to monitor the activity of the *Barx2* promoter in heterozygous and homozygous mutant tissues, and noticed a dramatic increase in X-Gal staining in *Barx2* mutant follicles at all phases of the hair cycle (Fig. 2 *A–C*) as well as in noncycling epithelia such as tongue (Fig. 2*D*). In telogen follicles, the most intense stain was restricted to the bulge of the follicle, the stem cell niche (Fig. 2*C*), which is consistent with a recent report on transcriptional profiling of label-retaining cells in skin (putatively the stem cells) that identified Barx2 as an enriched mRNA (31). In mutant skin, *Barx2-lacZ* reporter activity was further stimulated in the epidermis and nearby follicles during wound healing (Fig. 2*E*). By quantitative real-time PCR, the levels of intact 5′ Barx2 mRNA (which is present in both wild-type and mutant transcripts) were found to be ≈3-fold higher in knockout mice than in heterozygous or wild-type littermates (Fig. 2*F*). These data suggest an increase in *Barx2* promoter activity in the absence of functional Barx2.

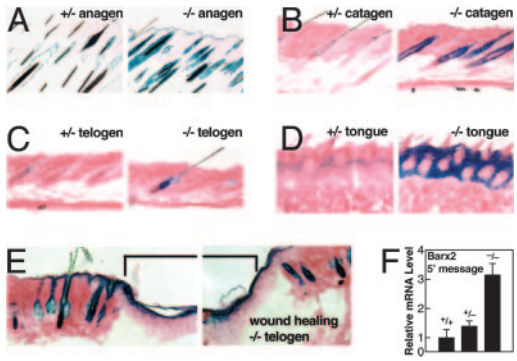


**Fig. 2.** Hyperactivity of *Barx2-lacZ* knock-in reporter in *Barx2* mutant tissue. (*A–E*) *Barx2* promoter activity detected by X-Gal staining, with control and mutant panels selected for approximately the same stage of the first hair cycle. (*A*) *Barx2* promoter activity is up-regulated in −/− outer root sheath and epidermis at P9. (*B*) Weak promoter activity in control but strong activity persists in −/− follicles during catagen at P19. (*C*) Only a few cells have detectable promoter activity in control telogen (at P19), but strong activity marks the bulge region in mutant telogen (at P21). (*D*) In noncycling epithelium of the tongue, *Barx2* promoter activity is increased in *Barx2*$^{-/-}$. (*E*) After 5 days of healing, the *Barx2-LacZ* reporter is stimulated in the epidermis, follicles, and sebaceous glands proximal to a wound (bracket). (*F*) Quantitative real-time PCR analysis of 5′*Barx2* mRNA levels normalized to *Gapdh*, indicating an increase in 5′*Barx2* message (common to both wild-type *Barx2* and *Barx2-lacZ* transcripts) in skin from *Barx2*$^{-/-}$ mice. Data represent the average of triplicate experiments with error bars for standard deviation from the mean.

To determine whether Barx2 could directly regulate its own expression, we examined the murine promoter and upstream sequences for binding sites. The *Barx2* promoter (12) does not contain any ATTA-cores indicative of homeodomain binding sites; however, ≈1.4 kb upstream from the translation start site, we identified a 160-bp element containing three putative Barx2 binding sites (Fig. 3*A*). Oligonucleotides encompassing two of the binding sites specifically interacted with GST-Barx2 protein when assayed *in vitro* by mobility shift (Fig. 7, which is published as supporting information on the PNAS web site). In cotransfection assays in primary keratinocyte cultures, full-length Barx2 repressed a reporter gene under the control of 2.43 kb of *Barx2* upstream promoter sequence (Fig. 3*B*). Similarly, a transcription unit regulated by the 160-bp element linked to the thymidine kinase promoter was repressed by cotransfection of Barx2 (Fig. 3*C*). A reporter gene with just 230 bp of *Barx2* minimal promoter was weakly repressed by Barx2 (2-fold repression, data not shown; compared to 5-fold repression of the −2.5-kb reporter gene, Fig. 3*B*), suggesting that the element between −1.6 and −1.4 kb is a primary, but not the only, means of *Barx2*-gene autorepression.

To examine the composition of factors on the 160-bp repressor element *in vivo*, we performed ChIP assays using formalin-fixed and homogenized anagen-stage skin and a specific Barx2 antibody. Barx2 was detected on the region encompassing the

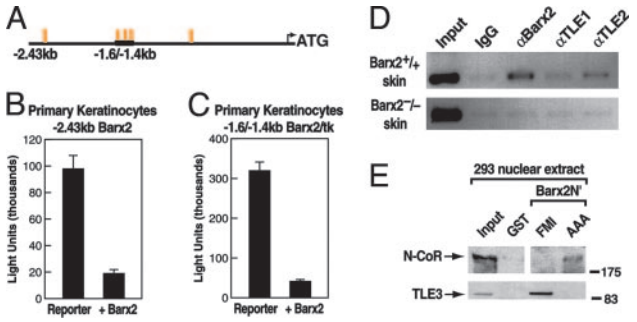


**Fig. 3.** Barx2 represses its own promoter. (*A*) Graphic depiction of five putative Barx2-binding sites (orange) over −2.43 kb of *Barx2* upstream sequence, with three sites within 160 bp between −1.6 and −1.4 kb (for actual sequence, see Fig. 7, which is published as supporting information on the PNAS web site). (*B* and *C*) Barx2 is a repressor on the 160-bp element: transient transfection reporter assays in primary keratinocytes with either the entire −2.43 kb (as in *A*), or just the 160-bp element with a thymidine kinase minimal reporter. (*D*) ChIP of Barx2 and TLE corepressors from skin, with PCR detection of the 160-bp element. The element is not detected in samples from Barx2$^{-/-}$ skin. Anti-TLE1 is specific for TLE1, whereas anti-TLE2 recognizes all TLEs. (*E*) Recruitment of corepressor proteins by the Barx2 N terminus: affinity chromatography using GST protein, GST-Barx2N′ (aa1–132) with wild-type eh-1 sequence (FMI), or with an eh-1 mutation (AAA). TLE3 and N-CoR were specifically purified from 293 cell nuclear extract, separated by SDS/PAGE, and identified by Western blot.

repressor element in samples from *Barx2*$^{+/+}$, but not *Barx2*$^{-/-}$, samples, and in addition, TLE corepressors were present on the 160-bp element in wild-type samples (Fig. 3*D*). Although we do not know the biological significance of Barx2 negative feedback autoregulation, given that it occurs during the hair cycle and can be stimulated as part of a wounding-healing response, it is tempting to speculate that these processes may be sensitive to expression levels of Barx2. As an example of this in the skin, Hoxc13, another homeodomain factor that exhibits negative autoregulatory feedback in the hair follicle (32), causes alopecia if its dosage is either increased in transgenic mice (32) or eliminated by targeted mutation (33).

Based on these observations for Barx2 autorepression, we explored the molecular mechanisms of Barx2-mediated repression. Barx2 contains a 7-aa eh-1 motif at amino acids 25–31 (see ref. 27), which is a well recognized motif for recruitment of TLE/Groucho corepressor complexes by homeodomain proteins. This complex of WD40-domain proteins can also function in a redundant fashion with other complexes, such as N-CoR corepressor complexes recruited, for example, by the homeodomain of several factors (34). We found a specific interaction between bacterially expressed GST-Barx2 N terminus (amino acids 1–132) and endogenous TLE3 protein present in nuclear extract from 293T cells, which was abolished with a mutation converting the FMI residues of the Barx2 eh-1 to alanines (Fig. 3*E*).

We found that the AAA form of Barx2 could interact with N-CoR in this system (Fig. 3*E*). N-CoR complexes have been described that contain additional F box/WD40-domain proteins, the transducin β-like factors, Tbl1 and TblR1 (20–23). In a second interaction system, we found that FLAG-Tbl1 was able to coimmunoprecipitate an N-terminally truncated Barx2 from which the first 40 aa, including the eh-1 motif, had been deleted. Binding to the truncated Barx2 was actually more effective than binding to the full-length Barx2 (Fig. 4*A*), suggesting the possibility of an open–closed conformation of the Barx2-Tbl1 complex, as has been noted for Tbl1 itself in its interactions with nuclear receptors (24). In transient transfection assays, we noted that the Barx2 N-terminal amino acids 1–132 include several independent regions besides the eh-1 that confer significant levels of repression when fused to the

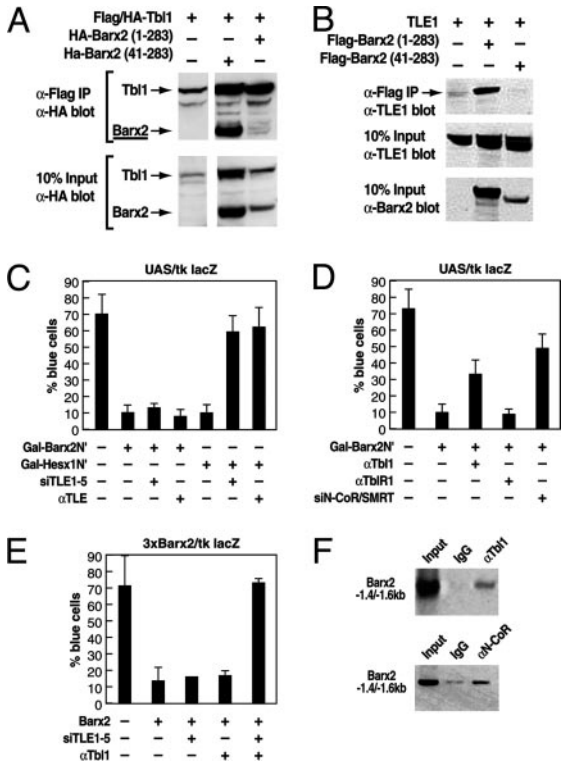


**Fig. 4.** Physical and functional interactions among Barx2, recruited corepressors, and *Barx2*-gene regulatory elements. (*A* and *B*) Proteins were coexpressed in 293 cells, and complexes were immunoprecipitated with anti-FLAG antibody. (*A*) Specific interaction between FLAG/HA-tagged Tbl1 and HA-tagged Barx2, with N-terminally truncated HA-Barx2 (second lane) interacting better than full-length HA-Barx2 (third lane). (*B*) Specific interaction between FLAG-Barx2 holoprotein and TLE1 (arrow), with full-length FLAG-Barx2 (second lane) interacting very well but no interaction with N-terminally truncated HA-Barx2 (third lane). (*C*) Plasmids, antibody, and a mixture of five siRNAs against mouse/rat TLEs1–5 were microinjected into nuclei of cultured cells and tested for Barx2-mediated repression of *lacZ* reporters. In Rat-1 cells, on UAS/tk promoter, TLEs are not required for repression by Gal-Barx2N′ (amino acids 1–132) fusion protein. Anti-TLE2 recognizes all TLEs. TLE antibody and TLE siRNA mixture are both effective at blocking repression by Gal-Hesx1N′. (*D*) Blocking N-CoR/SMRT or Tbl1 inhibits repression by the N terminus of Barx2. (*E*) In Rat-1 cells, on 3× multimerized Barx2 binding sites with a thymidine kinase (tk) promoter, the actions of both TLE and Tbl1 function in repression by full-length Barx2. (*F*) ChIP of corepressors from skin with PCR detection of the 160-bp element located at −1.6/−1.4 kb upstream of *Barx2*.

Gal4 DNA-binding domain (data not shown). A physical interaction between coexpressed Barx2 and TLE1 was again demonstrated by coimmunoprecipitation from 293T cells, and in contrast to the Barx2-Tbl1 interaction, deletion of the eh-1 motif abrogated this interaction (Fig. 4*B*). Therefore, the recruitment of TLEs and N-CoR:Tbl1 corepressor complexes occurs through distinct regions of the Barx2 N terminus.

We next wished to evaluate the functional importance of these interactions for Barx2-mediated repression. Curiously, TLE corepressors did not seem to be required for repression by the Barx2 N terminus, and single cell nuclear microinjection of a blocking pan-TLE antibody (15) or a mixture of siRNAs against TLE 1–5 had no effect on Gal-Barx2N′-mediated repression of a UAS/tk lacZ reporter in Rat-1 fibroblasts (Fig. 4*C*). For comparison, the same siRNAs and antibodies against TLE corepressors were fully effective in relieving eh-1-dependent repression by the N terminus of Hesx1 (Fig. 4*C*). In contrast, Gal-Barx2N′-mediated repression was relieved by single-cell nuclear microinjection of anti-Tbl1 antibody or by siRNAs

against N-CoR and SMRT (Fig. 4*D*). Antibody against TblR1 did not interfere with Barx2-mediated repression. Together, these data suggested context-specific functions of TLE and Tbl1 corepressors.

Therefore, we evaluated repression by Barx2 holoprotein, and found that neither TLE siRNAs nor anti-Tbl1 IgG was alone sufficient to block repressor function; however, by blocking the actions of both factors, we interfered with Barx2 repression activity on a reporter under the control of multimerized Barx2 binding sites (3xBarx2/tk lacZ) (Fig. 4*E*). Hence, although TLE complexes are recruited by eh-1 motifs found in many homeodomain factors, it appears that, for Barx2, this complex can either be redundant or cooperative with a second repressive activity that depends, in part, on Tbl1.

To explore whether these repressive activities represent direct effects, we performed ChIP assays from whole skin over the 160-bp repressor element of the *Barx2* gene with specific antibodies for Tbl1 and N-CoR, finding that both factors are recruited *in vivo* (Fig. 4*F*), similar to the TLE corepressors (Fig. 3*E*). The presence of Barx2 and its corepressors indicates that these complexes are likely to have functional relevance to Barx2 repression events *in vivo*, and reveals a role for both TLE and Tbl1 repression complexes on specific, repressed Barx2 gene targets, including the *Barx2* gene itself.

**Up-Regulated Genes Identified in *Barx2* Mutant Skin by RNA Profiling.** Based on its ability to act as a repressor, it became of particular interest to determine whether repression of additional, specific target genes might suggest a mechanism for the $Barx2^{-/-}$ phenotype. From a literature-based approach, we examined the expression levels of six important hair cycle regulators: *Fgf5* (30), *Tgfα* (35, 36), *Egf* (37), *PTHrP* (38), *Tgfβ1* (39), and *Msx2* (40). By quantitative real-time PCR before the onset of aberrant hair remodeling (day P11), we did not find significant changes in expression levels of these candidate genes between $Barx2^{-/-}$ and control tissue, although some of them actually decreased (relative to wild type) with the onset of catagen at P15 (data not shown). In contrast, we did find some other genes to be misexpressed at P11, after first identifying them by microarray profiling (see below). Therefore, these six known catagen-regulating genes might not be primary or direct targets of Barx2, but they may function elsewhere in the cascade leading to catagen.

The recent development of time-course gene expression profiling in the skin (6) has shown that the literature is far from complete with respect to the number of genes with hair-cycle associated expression patterns. Therefore, to broadly assay for gene changes caused by mutation of *Barx2*, we performed mRNA profiling by comparative microarray analysis using RNA isolated from back skin of mutant or control mice at P14, 1 day before catagen onset. Labeled RNA was hybridized with Affymetrix MG-U74Av2 chips, and we identified 45 differentially regulated transcripts representing 42 unique genes (see *Supporting Text* and Table 1, which is published as supporting information on the PNAS web site). Among these significant changes, *thrombospondin-1* (Tbs1) was up-regulated in *Barx2* mutant skin and bears a logical relationship to short hair in adult *Barx2* mutants, as it has been shown in an

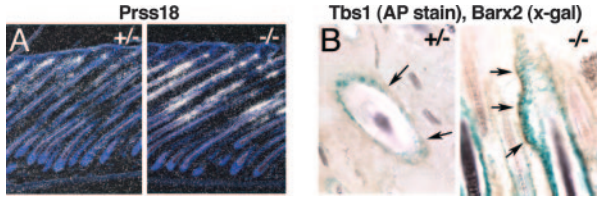


**Fig. 5.** Up-regulation of Prss18 and thrombospondin-1 in *Barx2* mutant hair follicles. (*A*) By *in situ* hybridization at day P14, *Prss18* mRNA is restricted to sebaceous gland and isthmus domain in control follicles, but is up-regulated in an expanded follicle domain in $Barx2^{-/-}$. (*B*) Double labeling at P14 of thrombospondin-1 (brown, alkaline phosphatase) and *Barx2-lacZ* reporter activity (X-Gal) in the outer root sheath, with up-regulation of both signals in $Barx2^{-/-}$. Arrows indicate specific AP stain.

earlier study that Tbs1 expression promotes the anagen–catagen transition in adult mice (41). However, it is unlikely that this single gene completely explains of the *Barx2* hair phenotype, because the earlier study used the keratin-14 promoter to overexpress Tbs1, and the level of up-regulation in *Barx2* mutants appears to be comparatively mild. The most up-regulated gene from the microarray was *Prss18* (neurosin/BSSP/zyme), encoding a secreted serine protease normally expressed in the sebaceous gland (42), which might be involved in the normal break down of inner root sheath as it dissociates from the hair shaft (1). However, its role in the biology of hair follicles is speculative, and its contribution to the *Barx2*-mutant phenotype awaits further investigation. Nonetheless, we confirmed that *thrombospondin-1* and *Prss18* were overexpressed in the follicles of $Barx2^{-/-}$ mice (Fig. 5), and we also noted that both genes contain Barx2-sites near their promoters (43, 44); therefore, they may be direct targets of Barx2 repression in the skin.

Overall, the mRNA changes on the microarray exhibited a preponderance of up-regulated genes over genes with decreased expression in *Barx2* mutants, with 34 of the 45 most highly significant changes in the up-direction, and five of the six most differential changes being overexpressed genes (Table 1). Most of these gene changes were also observed at P11, 3 days before the time of microarray profiling (Fig. 8, which is published as supporting information on the PNAS web site), confirming that they occur before the defect in hair remodeling. As putative Barx2 target genes, this pattern of gene up-regulation is consistent with our functional studies of Barx2 as a transcriptional repressor in the skin, and we suggest that the phenotypic consequences of *Barx2* mutation could be explained, in part, by the failure to repress critical gene targets.

We thank S. Yuspa and V. Virador for training on the isolation and culture of primary mouse keratinocytes, V. Perissi (University of California at San Diego, La Jolla) for reagents and technical assistance, F. Liu for ES cell culture and generation of chimeras, C. Nelson for cell culture, K. Park for hair measurements, the University of California at San Diego Center for AIDS Research genomics core laboratory for real-time PCR and microarray hybridizations, and J. Lozach for data analysis. L.E.O. was supported by 5T32DK007541. M.G.R. is an Investigator with the Howard Hughes Medical Institute. This work was supported by grants from the National Institutes of Health.

1. Stenn, K. S. & Paus, R. (2001) *Physiol. Rev.* **81,** 449–494.
2. Fuchs, E., Merrill, B. J., Jamora, C. & DasGupta, R. (2001) *Dev. Cell.* **1,** 13–25.
3. Paus, R. & Cotsarelis, G. (1999) *N. Engl. J. Med.* **341,** 491–497.
4. Cotsarelis, G. & Millar, S. E. (2001) *Trends Mol. Med.* **7,** 293–301.
5. Coulombe, P. A. (2003) *J. Invest. Dermatol.* **121,** 219–230.
6. Lin, K. K., Chudova, D., Hatfield, G. W., Smyth, P. & Andersen, B. (2004) *Proc. Natl. Acad. Sci. USA* **101,** 15955–15960.
7. Sander, G., Bawden, C. S., Hynd, P. I., Nesci, A., Rogers, G. & Powell, B. C. (2000) *J. Invest. Dermatol.* **115,** 753–756.
8. Saito, T., Sawamoto, K., Okano, H., Anderson, D. J. & Mikoshiba, K. (1998) *Dev. Biol.* **199,** 216–225.
9. Bulfone, A., Menguzzato, E., Broccoli, V., Marchitiello, A., Gattuso, C., Mariani, M., Consalez, G. G., Martinez, S., Ballabio, A. & Banfi, S. (2000) *Hum. Mol. Genet.* **9,** 1443–1452.
10. Tissier-Seta, J. P., Mucchielli, M. L., Mark, M., Mattei, M. G., Goridis, C. & Brunet, J. F. (1995) *Mech. Dev.* **51,** 3–15.
11. Jones, F. S., Kioussi, C., Copertino, D. W., Kallunki, P., Holst, B. D. & Edelman, G. M. (1997) *Proc. Natl. Acad. Sci. USA* **94,** 2632–2637.
12. Meech, R., Makarenkova, H., Edelman, D. B. & Jones, F. S. (2002) *J. Biol. Chem.* **278,** 8269–8278.
13. Smith, S. T. & Jaynes, J. B. (1996) *Development (Cambridge, U.K.)* **122,** 3141–3150.

14. Muhr, J., Andersson, E., Persson, M., Jessell, T. M. & Ericson, J. (2001) *Cell* **104,** 861–873.
15. Dasen, J. S., Barbera, J. P., Herman, T. S., O'Connell, S., Olson, L., Ju, B., Tollkuhn, J., Baek, S. H., Rose, D. W. & Rosenfeld, M. G. (2001) *Genes Dev.* **15,** 3193–3207.
16. Eberhard, D., Jimenez, G., Heavey, B. & Busslinger, M. (2000) *EMBO J.* **19,** 2292–2303.
17. Fisher, A. L. & Caudy, M. (1998) *Genes Dev.* **12,** 1931–1940.
18. Chen, G. & Courey, A. J. (2000) *Gene* **249,** 1–16.
19. Merrill, B. J., Gat, U., DasGupta, R. & Fuchs, E. (2001) *Genes Dev.* **15,** 1688–1705.
20. Guenther, M. G., Lane, W. S., Fischle, W., Verdin, E., Lazar, M. A. & Shiekhattar, R. (2000) *Genes Dev.* **14,** 1048–1057.
21. Yoon, H. G., Chan, D. W., Huang, Z. Q., Li, J., Fondell, J. D., Qin, J. & Wong, J. (2003) *EMBO J.* **22,** 1336–1346.
22. Tomita, A., Buchholz, D. R. & Shi, Y. B. (2004) *Mol. Cell. Biol.* **24,** 3337–3346.
23. Li, J., Wang, J., Wang, J., Nawaz, Z., Liu, J. M., Qin, J. & Wong, J. (2000) *EMBO J.* **19,** 4342–4350.
24. Perissi, V., Aggarwal, A., Glass, C. K., Rose, D. W. & Rosenfeld, M. G. (2004) *Cell* **116,** 511–526.
25. Dlugosz, A. A., Glick, A. B., Tennenbaum, T., Weinberg, W. C. & Yuspa, S. H. (1995) *Methods Enzymol.* **254,** 3–20.
26. Krasner, A., Wallace, L., Thiagalingam, A., Jones, C., Lengauer, C., Minahan, L., Ma, Y., Kalikin, L., Feinberg, A. P., Jabs, E. W., *et al.* (2000) *Gene* **250,** 171–180.
27. Herring, B. P., Kriegel, A. M. & Hoggatt, A. M. (2001) *J. Biol. Chem.* **276,** 14482–14489.
28. Jepsen, K., Hermanson, O., Onami, T. M., Gleiberman, A. S., Lunyak, V., McEvilly, R. J., Kurokawa, R., Kumar, V., Liu, F., Seto, E., *et al.* (2000) *Cell* **102,** 753–763.
29. Muller-Rover, S., Handjiski, B., van der Veen, C., Eichmuller, S., Foitzik, K., McKay, I. A., Stenn, K. S. & Paus, R. (2001) *J. Invest. Dermatol.* **117,** 3–15.
30. Hebert, J. M., Rosenquist, T., Gotz, J. & Martin, G. R. (1994) *Cell* **78,** 1017–1025.
31. Tumbar, T., Guasch, G., Greco, V., Blanpain, C., Lowry, W. E., Rendl, M. & Fuchs, E. (2004) *Science* **303,** 359–363.
32. Tkatchenko, A. V., Visconti, R. P., Shang, L., Papenbrock, T., Pruett, N. D., Ito, T., Ogawa, M. & Awgulewitsch, A. (2001) *Development (Cambridge, U.K.)* **128,** 1547–1558.
33. Godwin, A. R. & Capecchi, M. R. (1998) *Genes Dev.* **12,** 11–20.
34. Xu, L., Lavinsky, R. M., Dasen, J. S., Flynn, S. E., McInerney, E. M., Mullen, T. M., Heinzel, T., Szeto, D., Korzus, E., Kurokawa, R., Aggarwal, A. K., Rose, D. W., Glass, C. K. & Rosenfeld, M. G. (1998) *Nature* **395,** 301–306.
35. Hansen, L. A., Alexander, N., Hogan, M. E., Sundberg, J. P., Dlugosz, A., Threadgill, D. W., Magnuson, T. & Yuspa, S. H. (1997) *Am. J. Pathol.* **150,** 1959–1975.
36. Murillas, R., Larcher, F., Conti, C. J., Santos, M., Ullrich, A. & Jorcano, J. L. (1995) *EMBO J.* **14,** 5216–5223.
37. Mak, K. K. & Chan, S. Y. (2003) *J. Biol. Chem.* **278,** 26120–26126.
38. Cho, Y. M., Woodard, G. L., Dunbar, M., Gocken, T., Jimenez, J. A. & Foley, J. (2003) *J. Invest. Dermatol.* **120,** 715–727.
39. Foitzik, K., Lindner, G., Mueller-Roever, S., Maurer, M., Botchkareva, N., Botchkarev, V., Handjiski, B., Metz, M., Hibino, T., Soma, T., *et al.* (2000) *FASEB J.* **14,** 752–760.
40. Ma, L., Liu, J., Wu, T., Plikus, M., Jiang, T. X., Bi, Q., Liu, Y. H., Muller-Rover, S., Peters, H., Sundberg, J. P., *et al.* (2003) *Development (Cambridge, U. K.)* **130,** 379–389.
41. Yano, K., Brown, L. F., Lawler, J., Miyakawa, T. & Detmar, M. (2003) *J. Invest. Dermatol.* **120,** 14–19.
42. Meier, N., Dear, T. N. & Boehm, T. (1999) *Biochem. Biophys. Res. Commun.* **258,** 374–378.
43. Shingu, T. & Bornstein, P. (1994) *J. Biol. Chem.* **269,** 32551–32557.
44. Matsui, H., Kimura, A., Yamashiki, N., Moriyama, A., Kaya, M., Yoshida, I., Takagi, N. & Takahashi, T. (2000) *J. Biol. Chem.* **275,** 11050–11057.